https://doi.org/10.5194/cp-2021-144
Preprint. Discussion started: 18 November 2021

Climate of the Past Discussions
Open Access
EGU

An Intertropical Convergence Zone shift controlled the terrestrial material supply on the Ninetyeast Ridge

Xudong Xu[1,2,3], Jianguo Liu[1,2,4,], Yun Huang[1,*], Lanlan Zhang[1,2], Liang Yi[4,5], Shengfa Liu[4,6], Yiping Yang[1,2], Li Cao[1,2,3], Long Tan[1,2,3]*

[1]Key Laboratory of Ocean and Marginal Sea Geology, South China Sea Institute of Oceanology, Innovation Academy of South China Sea Ecology and Environmental Engineering, Chinese Academy of Sciences, Guangzhou 510301, China

[2]Southern Marine Science and Engineering Guangdong Laboratory (Guangzhou), Guangzhou 511458, China

[3]University of Chinese Academy of Science, Beijing 100049, China

[4]Laboratory for Marine Geology, Qingdao National Laboratory for Marine Science and Technology, Qingdao 266061, China

[5]State Key Laboratory of Marine Geology, Tongji University, Shanghai 200092, China

[6]Key Laboratory of Marine Geology and Metallogeny, First Institute of Oceanography, Ministry of Natural Resources, Qingdao 266061, China

Corresponding authors: Jianguo Liu (jgliu@scsio.ac.cn) and Yun Huang (huangyun@scsio.ac.cn)

Abstract

Among various climate drivers, direct evidence for the Intertropical Convergence Zone (ITCZ) control of sediment supply on the millennium scale is lacking, and the changes in ITCZ migration demonstrated in paleoclimate records need to be better investigated. Here, we use clay minerals and Sr-Nd isotopes obtained from a gravity core on the Ninetyeast Ridge to track the corresponding source variations and analyze the relationship between terrestrial material supplementation and climatic changes. On the glacial-interglacial scale, chemical weathering weakened during the North Atlantic cold climate periods, and falling sea level hindered the transport of smectite into the study area due to the exposure of islands. However, the influence of the South Asian monsoon on the sediment supply was not obvious on the millennium scale. We suggest that the north-south migration of the ITCZ controlled the rainfall in Myanmar and further directly determined the supply

https://doi.org/10.5194/cp-2021-144
Preprint. Discussion started: 18 November 2021

Climate of the Past Discussions

of clay minerals on the millennium scale because the transport of smectite was highly connected with ITCZ location. Furthermore, the regional shift of the ITCZ induced an abnormal increase in the smectite percentage during the late Last Glacial Maximum (LGM) in our records. The smectite percentage in the studied core is similar to distinct ITCZ records in different time periods, revealing that regional changes in the ITCZ were significantly obvious, and that the ITCZ is not a simple N-S displacement and closer connections occurred between the Northern-Southern Hemispheres in the eastern Indian Ocean during the late Last Glacial Maximum (LGM).

1. Introduction

Deposited sediments are essential recorders of the paleoclimate and paleo-ocean since the climate is tied to the whole sedimentation process, from weathering and transport to the deposition of sediments on land. The terrestrial materials of "source-sink" systems are supplied to marine environments under the combined effects of multiple climate-related driving forces and ocean processes (Li et al., 2018; Yu et al., 2019), and understanding these effects is crucial for reconstructing coevolutionary relationship of the paleoenvironment with the paleo-oceans and paleoclimate. Various factors may control the formation and transport of terrestrial materials at low latitudes such as the northeastern Indian Ocean. Recently, the South Asian monsoon has been revealed to be the main driving force of terrestrial material supply in Bangladesh and of hydrological changes in the Bay of Bengal (BoB, Dutt et al. al., 2015; Gebregiorgis et al., 2016; Joussain et al., 2017; Li et al., 2018; Liu et al., 2021). Moreover, the Intertropical Convergence Zone (ITCZ) is a nonnegligible climate-driving force in low-latitude regions (Deplazes et al., 2013; Ayliffe et al., 2013), which has its pivotal role in the heat transportation on earth (Schneider et al., 2014) and the north-south shift of the ITCZ is thought to connect the climates in the Northern and Southern Hemispheres (Huang et al., 2019; Zhuravleva et al., 2021). Because the monsoon dynamics are shaped by large-scale meridional temperature gradients and an ITCZ shift in tropical monsoon area (Mohtadi et al., 2016), there are hopeful opportunities to analyze sediment response to the ITCZ or monsoon. Evidence for direct control of terrestrial sediment supply by the ITCZ remains lacking, which is an obstacle to understanding the response of the depositional

https://doi.org/10.5194/cp-2021-144
Preprint. Discussion started: 18 November 2021

Climate of the Past Discussions
Open Access
EGU

environment to the ITCZ shift. However, the paleoclimate breakthroughs mentioned above enable us to analyze the response of sedimentary records to the ITCZ shift in the BoB more accurately.

As the main deposition area for vast amounts of weathered Himalayan materials, the BoB accumulates numerous Himalayan terrestrial materials that are loaded by the Ganges-Brahmaputra (G-B) River (Goodbred and Kuehl, 2000) and forms the largest subaqueous fan-Bengal Fan (3000 km long from north to south, 1400 km wide from east to west, with an area of 3.9×10^5 km^2; Curray et al., 2002).The eastern and western sides of the BoB correspond to the Andaman Sea and the Indian Peninsula, respectively, and the BoB is a natural site that is useful for studying the interactions between weathering and climatic factors since both sides of the bay are affected by the South Asian monsoon (Ali et al., 2015). Over the past twenty years, the sediment provenance in the BoB during the late Quaternary has been discussed as a hot topic, especially the provenance of sediments in the Andaman Sea (Ali et al., 2015; Awasthi et al., 2014) and in the northern (Li et al., 2018; Ye et al., 2020), western (Kessarkar et al., 2005; Tripathy et al., 2011; Tripathy et al., 2014) and eastern (Colin et al., 1999; Colin et al., 2006; Joussain et al., 2016) parts of the BoB. However, little attention has been given to sediment provenance in the southern BoB or, particularly, to the correlation of these sediment sources with climatic driving factors. Recent studies have revealed that clay minerals can be used to effectively track changes in source areas in the source-sink system of the BoB due to the great differences in clay mineral components among the source areas around the BoB (Joussain et al., 2016; Li et al., 2017; Liu et al., 2019a; Ye et al., 2020). Moreover, Sr-Nd isotopes have been widely reported to track the variations of sediment provenance in the BoB (Ahmad et al., 2005; Colin et al., 1999; Colin et al., 2006).

In this study, we measured clay minerals and Sr-Nd isotopes in a deep-sea gravity core obtained from the southeastern BoB (Figure 1) to reconstruct variations in the sources of sediments in the Ninetyeast Ridge and to further explore the climate forces that affected the supply of terrestrial materials during the past 45 ka. The Ninetyeast Ridge is far from the G-B river estuary and much shallower than the underwater Bengal Fan, which makes the terrestrial sediments on the Ninetyeast Ridge suitable for exploring the relationship between the paleoclimate and paleoenvironment in the BoB. We

https://doi.org/10.5194/cp-2021-144
Preprint. Discussion started: 18 November 2021


Climate of the Past Discussions
Open Access
EGU

aim to disentangle the ITCZ variability signal in marine sediments from multiple driving forces and further understand the response of sedimentary records to the ITCZ migrations.

2. Material and methods

2.1. Chronology

The gravity core 17I106 (90.0040°E, 6.2105°N, water depth 2928 m) was collected by the *R/V Shiyan 1* vessel belonging to the South China Sea Institute of Oceanology (SCSIO), Chinese Academy of Sciences (CAS), from the Ninetyeast Ridge, northeast of the Indian Ocean (Figure 1). This core has a total length of 162 cm and consists of gray to green silty clays subsampled at 1-cm intervals. The age model of core 17I106 was reconstructed based on 10 accelerator mass spectrometry (AMS) ^{14}C dates and Bayesian interpolations between these dates (Figure 2 and Table 1). AMS ^{14}C dating was performed on mixed planktonic foraminifera at Beta Analytic Inc. More than 20 mg of intact mixed planktonic foraminifera shells were selected from the >150 μm fractions of each sample (10 g dried sample). All radiocarbon ages were converted and reported as calendar years before present with the Calib8.2 software program with the Marine20 calibration dataset (Reimer et al., 2020). A continuous depth-age model was performed using Bacon software by dividing a sedimentary sequence into many thin segments and estimating a linear accumulation rate for each segment based on the calibrated ^{14}C dates and a Bayesian approach (Blaauw and Christen, 2011).

2.2. Clay mineralogy

Clay minerals (<2 μm) were separated from the sediment samples according to Stokes' settling velocity principle after organic materials and carbonates were removed with 15% hydrogen peroxide (H_2O_2) and 0.1 N chlorohydric acid (HCl), respectively. The clay mineral slides were measured using routine X-ray diffraction (XRD) equipment (Bruker Inc, D8 ADVANCE) in the Key Laboratory of Ocean and Marginal Sea Geology, SCSIO, CAS. Clay mineral abundance was calculated by measuring the peak areas of smectite (15-17 Å), illite (10 Å) and kaolinite/chlorite (7 Å). Relative proportions

https://doi.org/10.5194/cp-2021-144
Preprint. Discussion started: 18 November 2021


Climate of the Past Discussions
Open Access
EGU

of kaolinite and chlorite were calculated from the ratio of 3.57 Å/3.54 Å peak areas. The relative percentages of the four main clay minerals were estimated by calculating the integrated peak areas of characteristic basal reflections using Topas5P software with the empirical factors by Biscaye (1965). The reproducibility error of this method is ± 5-10%.

2.3 Sr-Nd isotope analyses

22 samples from core 17I106 were selected for isotope analyses. Strontium (Sr) and neodymium (Nd) isotopic compositions of the sediment samples were measured using a Thermo Scientific Multi-Collector Inductively Coupled Plasma Mass Spectrometer (MC-ICPMS Nu plasma) at the Key Lab of Marine Sedimentology and Environmental Geology, Ministry of Natural Resources, China. The organic materials and carbonate were removed from the samples by H2O2 and HCl, respectively. For the convenience of direct comparison, the Nd isotopic ratio results are expressed as εNd (0)=[(143Nd/144Nd)meas/0.512638-1]*10000, using the present CHUR value (Jacobsen et al, 1980). Replicate analyses of NBS-987 during the study gave a mean 87Sr/86Sr of 0.710310 ± 0.000003 (2s), close to its certified value of 0.710245. Similarly, replicate analyses of JNDi-1 gave a mean 143Nd/144Nd of 0.512112 ± 0.000004 (2s), and its certified value is 0.511860.

3. Results

The age model is built based on 10 radiocarbon dates of core 17I106. The top age is 3.8ka BP and bottom age is 44.9 ka BP, thus this core covers a continuous sedimentary succession of the last ~45000 years. The sedimentation rates in the Holocene (average 3.1 cm/ka) were relatively lower than those during the last glacial period (average 4.6 cm/ka), with the highest rate of 8.3 cm/ka during 12.5–13.6 ka BP (Figure 3a). In the study core, illite percentage ranges from 31% to 63% with an average of 48%, while smectite, percentage ranges between 8% and 57%, with an average of 30% (Figure 3b-e). Moreover, kaolinite percentage ranges from 2% to 16%, and chlorite percentage ranges from 5% to 20% in the core sediments. In the study core, the $^{87}Sr/^{86}Sr$ ratios range from 0.7122015 to 0.7186141 with an average of 0.7161698, while

https://doi.org/10.5194/cp-2021-144
Preprint. Discussion started: 18 November 2021


Climate of the Past Discussions

εNd values range from -13.02 to -10.29, with an average of -11.24 (Figure 3). At this study core, the $^{87}Sr/^{86}Sr$ ratio and εNd values stay stable before the LGM but show fluctuations after the LGM, without obvious increasing/decreasing tendencies. During ~14.5-12.5 ka, $^{87}Sr/^{86}Sr$ ratios significantly increased from 0.7139 to 0.7172, while εNd values decreased abruptly from -10.28 to -13.02.

4. Discussion

4.1. Sediment provenance and transport patterns

The lower sedimentation rates (3-5 cm/ka) measured in core 17I106 were in accordance with the normal sedimentation rates obtained from cores SK157-14, SK157-15 and SK157-16 around the Ninetyeast Ridge (Ahmad et al., 2005; Raza et al., 2013). In this region, turbidite activities were less developed (Joussain et al., 2016; Fournier et al., 2017), in accordance with its far distance from the Active Channel. In the northern BoB, due to heavy river runoff and steep topography, the G-B river system transports a large amount of the products of Himalayan physical denudation; these products mainly consist of illite and chlorite formed under dry and cold climate conditions (Chamley, 1989; Khan et al., 2019). Because of the hot and humid conditions in Myanmar and the Indian Peninsula, sediments in these regions are formed through the chemical weathering of silicate minerals and thus have high smectite percentages. Moreover, the Irrawaddy River brought weathered products characterized by high smectite percentage from Myanmar into the Andaman Sea, leading to high smectite percentages in the terrestrial sediments deposited in this marine environment (Ali et al., 2015).

The relatively high illite percentages measured in core 17I106 indicate that the weathered Himalayan materials carried by the G-B River system are the primary source of sediments in the study area (Figure 4a). Compared with the large amounts of materials loaded by the G-B River system, the weathered areas and runoff volumes of the Indo-Burman Ranges are relatively small, and consequently, their sediment contributions are limited in the study area, although their sediments are also characterized by relatively high illite percentages (Joussain et al., 2016). Evidence of surface sediments in the BoB

https://doi.org/10.5194/cp-2021-144
Preprint. Discussion started: 18 November 2021

Climate of the Past Discussions

further reveal that the smectite percentages of sediments in the central region are significantly lower than those in the eastern and western regions (Li et al., 2017; Liu et al., 2019a), indicating that sediments of Indian Peninsula origin are difficult to transport into the eastern BoB through the central BoB. Because the limited weathering area of Andaman-Nicobar islands cannot provide a large amount of smectite according to provenance studies (Ali et al., 2015), the Myanmar materials characterized by high smectite percentages have the advantage of shorter transport distances compared to those sourced from the Indian Peninsula as the main source area of smectite around the BoB, Therefore, the most important source of smectite in the study area is the Myanmar region. In marine environments, kaolinite is preferentially deposited in estuary areas due to mineral segregation (Gibbs, 1977) and thus cannot be transported over long distances, so the kaolinite in the study area was most likely sourced from neighboring Sumatra (Figure 4a, Liu et al., 2012). The Sr-Nd isotopes measured in the studied core are close to those measured in the Irrawaddy/Indo-Burman Ranges/Sumatra source regions (Figure 4b), indicating that terrestrial materials with diameters <63 μm mainly come from the Irrawaddy River, Indo-Burman Ranges and the Sumatra source areas; these source areas are closer to the study area than the G-B River system, as was confirmed by a Sr-Nd isotope study in the southwestern part of the study area (Ahmad et al., 2005). This result is not consistent with the evidence provided by clay minerals, which indicate that the Himalayas were the main sediment source. This difference may be consistent with the view that clay minerals may be transported over long distances while coarser terrestrial sediments can only be transported to more proximate locations.

In the northeastern BoB, the southwest monsoon turns southward into the Andaman Sea, resulting in the transport of sediments from the Indo-Burman Range and Irrawaddy River to the central Andaman Sea (Colin et al., 2006). The location of core 17I106, drilled on the Ninetyeast Ridge, was above the normal seafloor, and the terrestrial materials deposited to the west of this location are difficult to resuspend and deposit on the ridge under the force of bottom currents or turbidity. In fact, G-B materials are mainly carried eastward by surface ocean currents in summer to the Andaman Sea, where the seasonal surface currents load materials from the Himalayan and Indo-Burman Ranges into the Andaman Sea through the

https://doi.org/10.5194/cp-2021-144
Preprint. Discussion started: 18 November 2021


Climate of the Past Discussions
Open Access
EGU

152 northern strait (NS) (Figure 5, Liu et al., 2020a; Rayaroth et al., 2016); then, a westward ocean current in the middle strait
153 (MS) loads sediments southwest into the study area (Chatterjee et al., 2017).

154 **4.2. Factors affecting sediment provision**

155 In general, illite is the major mineral produced during the strong physical erosion of metamorphic rocks and granite rocks
156 and during the reprocessing of sedimentary rocks (Chamley, 1989; Winkler et al., 2002), while smectite is the secondary
157 mineral produced during the chemical weathering of parent aluminosilicate and iron-magnesium silicate under warm and
158 humid climate conditions (Chamley, 1989; Erosion, 1995). The climatic forces from the North Atlantic are thought to
159 extensively impact the tropical Eastern Indian Ocean (EIO) and surrounding areas in the BoB (DiNezio and Tierney, 2013;
160 Dutt et al., 2015; Gautam et al., 2020; Mohtadi et al., 2014; Peng et al., 2019; Liu et al., 2021). During the North Atlantic
161 cold-climate periods (Heinrich events and YD period, Figure 3h) when rainfall and temperatures decreased, physical
162 weathering was enhanced in the Himalayas (Joussain et al., 2016) while chemical weathering weakened in Myanmar and
163 the smectite percentage thus decreased in the source area.

164 Sea level fluctuation is also critical in controlling the supplementation of terrestrial materials, especially clay minerals
165 (Li et al., 2018; Liu et al., 2019a), by changing the transport paths and/or distances as well as the further input of sediments
166 into the study area. The changing trends of the sea level in seas adjacent to the BoB (Figure 3i, Waelbroecka et al., 2002;
167 Grant et al., 2014; Hanebuth et al., 2000; Thompson and Goldstein, 2006) are well correlated with the smectite percentages
168 measured in core 17I106, especially during 35-21 ka, when the smectite percentages declined continuously. Since the
169 Andaman-Nicobar Islands connecting the Andaman Sea and the BoB have continuously expanded as the sea level has
170 continuously declined, the strait width has been consistently reduced, thereby preventing the entrance of terrestrial
171 materials in the Andaman Sea and the further continuous decline in smectite percentages in the study area. Here, we suggest
172 that the variations in the measured illite percentages were mainly caused by changes in smectite deposition because the

https://doi.org/10.5194/cp-2021-144
Preprint. Discussion started: 18 November 2021


Climate of the Past Discussions
Open Access
EGU

173 sedimentary records obtained from the northern BoB do not support the controlling effect of the sea level on illite
174 percentages over the past 50 ka (Joussain et al., 2016; Li et al., 2018; Liu et al. al., 2019a).

175 The South Asian summer monsoon is normally thought to be an important factor affecting weathering conditions
176 around the BoB (Dutt et al., 2015; Gebregiorgis et al., 2016; Joussain et al., 2017; Li et al., 2018; Rashid et al., 2011; Zhang
177 et al., 2020; Zorzi et al., 2015). Stalagmites in Mawmluh Cave record variations in river runoff in the surrounding area;
178 these variations are determined by the impacts of SST and water vapor transport paths (Dutt et al., 2015). In fact, the
179 Mawmluh Cave records of the South Asian monsoon strength are driven by temperature gradients which drive changes in
180 winds and moisture transport into BoB (Dutt et al., 2015), not just response to the rainfall amount. The smectite percentage
181 changes measured in core 17I106 were slightly correlated after Heinrich event 1(H1) but were irrelevant before H1 (Figure
182 6b). This indicated the combination of temperature and moisture failed to play crucial role in smectite importation to core
183 17I106 though weathering features in the source area may be shaped by the South Asian monsoon. Moreover, the view
184 could be confirmed by the smectite record obtained from the studied core was not well-correlated with records previously
185 obtained in the Andaman Sea (Figure 6c,6d, Gebregiorgis et al., 2016) or with a sporopollen record obtained in Southwest
186 China (Figure 6e,6f, Zhang et al., 2020), especially before the LGM. The consistency of salinity, SST in core SK 168
187 (Figure 6c,6d) and moisture, temperature Index (Figure 6e,6f) in Southwest China reveal the hydroclimate in the South
188 Asian monsoon region might have been influenced by SST in the Indian Ocean. All these inconsistencies between smectite
189 percentage in core 17I106 and monsoon records indicate that smectite supplementation may be mainly controlled by rainfall
190 rather than by chemical weathering due to thermodynamic differences between sea and land environments (Liu et al.,
191 2020b).

192 During the late LGM, the smectite percentage increased abnormally in core 17I106, and this increase cannot be
193 explained by dry and cold weathering conditions, a lower sea level or a weakened summer monsoon at that time. In contrast,
194 this abnormal change may have been attributed to an increase in the smectite input in sediments from the Burman source

https://doi.org/10.5194/cp-2021-144
Preprint. Discussion started: 18 November 2021


Climate of the Past Discussions
Open Access
EGU

195 area or to a decrease in the amounts of sediments input from the Himalayas. Under the influence of the winter monsoon
196 during the LGM, the denudated sediments on the Irrawaddy Estuary shelf may have been transported southward through
197 the west side of Andaman Island (Prajith et al., 2018), as was confirmed in previous work showing that the winter monsoon
198 led to an increase in terrestrial materials from the Irrawaddy River to the Ninetyeast Ridge during the Heinrich event
199 (Ahmad et al., 2005). However, the winter monsoon was strong in the west of the study area from 21 to 15 ka (Figure 6g),
200 and the sea level remained relatively low during that period (Gautam et al., 2020). The smectite percentages in the studied
201 core increased significantly from 21 to 19 ka and dropped rapidly after 19 ka. This inconsistency contradicts the conclusion
202 that the increased smectite percentage in the source area was caused by a strong winter monsoon. Moreover, the changes
203 in the sediment compositions measured in the Himalayan source area were probably related to variations in regional glaciers.
204 During the LGM period, the increased glacial cover may have reduced surface runoff and furthered the transport of physical
205 weathering products, while the increased amount of ice meltwater may have transported more illites following glacial melt.
206 However, the reduced glacial area in the Himalayas during 18-15ka did not occur simultaneously with the increased illite
207 percentage (Yan et al., 2020; Weldeab et al., 2019, Figure 6h). Therefore, the abnormal changes measured in the smectite
208 percentage during the late LGM period were caused by other climate-driven mechanisms, and the millennium-scale
209 smectite percentage fluctuations that occurred before the LGM require a more reasonable explanation.

210 **4.3. The ITCZ shift in the EIO**

211 Changes in rainfall and the corresponding runoff are generally utilized to explain short-term variations in clay minerals. In
212 the EIO, rainfall is controlled by monsoon activities (An et al., 2011; Beck et al., 2018; Gebregiorgis et al., 2016) and/or
213 ITCZ migrations (Deplazes et al., 2013; Stoll et al., 2007; Tan et al., 2019). As a climate-driving force in low-latitude
214 regions, ITCZ migrations may be the main factor responsible for regional hydrological changes. During the glacial-
215 interglacial period, the ITCZ migrated north-south and balanced thermal differences by transferring atmospheric heat; this
216 process represents an indispensable climate-regulating power on earth (Broccoli et al., 2006; McGee et al., 2018; Schneider

https://doi.org/10.5194/cp-2021-144
Preprint. Discussion started: 18 November 2021


Climate of the Past Discussions
Open Access
EGU

et al., 2014). In the Cariaco Basin and Arabian Seas (Figure 7), tropical rainfall is highly correlated with the North Atlantic climate, and sea ice variations in the North Atlantic affect the north-south shift of the ITCZ in low-latitude regions through atmospheric circulation and ocean processes (Deplazes et al., 2013). The smectite particles measured in core 17I106 mainly came from the Myanmar source area; in this area, rainfall is greatly affected by the seasonal shift of the ITCZ. Before the LGM, the smectite percentages in the study core were well-matched with the ITCZ record in the Arabian Sea (Deplazes et al., 2013). The supplement of smectite percentages reached the peak when ITCZ shifted significantly northernmost according to record of Arabian Sea. And during cold-climate events when the ITCZ moved significantly southward, rainfall decreased, the smectite percentages decreased correspondingly in the source area. Therefore, we suggest that these changes in the smectite percentages in the studied core are correlated with ITCZ migration and the rainfall is an important factor determining the smectite percentage from the source area of Myanmar.

Although the changes in smectite percentages in the study area are associated with ITCZ shifts before and after the LGM, the ITCZ shift in the Indo-Pacific warm pool (IPWP) was more “regional” than those in the Arabian Sea and the Cariaco Basin (Deplazes et al., 2013). During the late LGM, when the ITCZ did not move extensively in the Arabian Sea, the ITCZ gradually shifted northward in the IPWP from 21-18 ka (Figure 7, Ayliffe et al., 2013). However, the smectite percentage increased significantly in the study area, and we have excluded the possibility that the winter monsoon or meltwater influenced these changes. Further comparisons with IPWP records reveal that the ITCZ changes agree well with the smectite percentage variations during the late LGM, indicating that the northern migration of the ITCZ induced high smectite percentages in core 17I106. The smectite percentage in the studied core is similar to distinct ITCZ records in different time periods, revealing that regional changes in the ITCZ were significantly obvious, which propose the ITCZ is not a simple N-S displacement. This consistency may indicate that the regional extension of the north-south thermodynamic gradient in the EIO exceeded that in the Arabian Sea and that the north-south shift of the ITCZ caused the climate systems of the Northern and Southern Hemispheres to be more closely connected in the EIO during the late LGM (Huang et al.,

https://doi.org/10.5194/cp-2021-144
Preprint. Discussion started: 18 November 2021

2019; Zhuravleva et al., 2021). These factors may be correlated with observed variations in regional air-sea interactions, such as the exposure of the Sunda Shelf (DiNezio and Tierney, 2013) and the effect of the thermocline in the EIO (Mohtadi et al., 2017). Thus, the regional variations in the ITCZ should be fully considered when studying climate change, especially in low-latitude regions that are sensitive to environmental changes, such as the EIO (Niedermeyer et al., 2014).

5. Conclusion

We reconstructed the variations in sediment sources on the Ninetyeast Ridge over the past 45 ka. The main source areas comprise the Himalayan and Irrawaddy River; sediments were stably supplied from these regions throughout the studied core. When North Atlantic cold events occurred, chemical weathering weakened and physical weathering increased; correspondingly, the smectite percentage decreased and the illite percentage increased. From 35-21 ka, the falling sea level led to an increase in the exposed area of the Andaman-Nicobar Islands and further hindered the entrance of smectite from the Andaman Sea into the study area. At the same time, the influence of the South Asian monsoon on the sediment supply was not obvious. The time-phase mismatches observed among records excluded the influence of Burman shelf sediment erosion forced by the winter monsoon or of variations in G-B river sediments induced by ice meltwater on the abnormal increases observed in the smectite percentages during the late LGM. The smectite record of core 17I106 is consistent with the ITCZ changes recorded on the millennium scale, indicating that the ITCZ controls the rainfall in the Burman source area and, further, the clay mineral variations in the study area. The inferred ITCZ shift recorded in the studied core coincided with the global ITCZ change that occurred before the LGM, but during the late LGM, the core record was consistent with the change in the regional ITCZ recorded in the EIO, indicating that the regional ITCZ was significantly connected with the Northern-Southern Hemispheres.

Author contributions.

J.L. and Y.H. conceived and designed the experiment. X.X. wrote the manuscript with contributions from all authors. L.Z.

and L.Y. provided the ages of planktonic foraminifera, and S.L., Y.Y., L.C., and L.T. helped to analyze the measured data and discuss the related relevant topics of in this manuscript.

Competing interests.

The authors declare that they have no conflict of interest.

Acknowledgements.

We thank Hui Zhang for Sr-Nd isotope measurements. Core sediment samples were collected on board of R/V "Shiyan 1" implementing the open research cruise NORC 2012-08 supported by NSFC Shiptime Sharing Project.

Financial support.

This work has been jointly funded by the National Nature Science Foundation of China (42176075 and 41576044), Key Special Project for Introduced Talents Team of Southern Marine Science and Engineering Guangdong Laboratory (Guangzhou) (GML2019ZD0206), and the Strategic Priority Research Program of the Chinese Academy of Sciences (XDB42000000).

Data Availability Statement.

All dataset is available on Science Data Bank (https://www.scidb.cn/detail?dataSetId=55c7dcf1f8344c658099dfe030264b2f).

References

Ahmad, S. M., Anil Babu, G., Padmakumari, V. M., Dayal, A. M., Sukhija, B. S., and Nagabhushanam, P.: Sr, Nd isotopic evidence of terrigenous flux variations in the Bay of Bengal: Implications of monsoons during the last ~34,000 years, Geophys. Res. Lett., 32, L22711, https://doi.org/10.1029/2005GL024519, 2005.

Ahmad, S. M., Padmakumari, V. M. and Babu, G. A.: Strontium and neodymium isotopic compositions in sediments from

https://doi.org/10.5194/cp-2021-144
Preprint. Discussion started: 18 November 2021

280 Godavari, Krishna and Pennar rivers, Curr. Sci., 97, 1766-1769, 2009.

281 Ali, S., Hathorne, E. C., Frank, M., Gebregiorgis, D., Stattegger, K., Stumpf, R., Kutterolf, S., Johnson, J. E., and Giosan,
282 L.: South Asian monsoon history over the past 60 kyr recorded by radiogenic isotopes and clay mineral assemblages
283 in the Andaman Sea, Geochem., Geophys., Geosy., 16, 505-521, https://doi.org/10.1002/2014gc005586, 2015.

284 An, Z., Clemens, S., Shen, J., Qiang, X., Jin, Z., Sun, Y., Prell, W., Luo, J., Wang, S., Xu, H., Cai, Y., Zhou, W., Liu, X.,
285 Liu, W., Shi, Z., Yan, L., Xiao, X., Chang, H., Wu, F., Ai, L., and Lu, F.: Glacial-Interglacial Indian Summer Monsoon
286 Dynamics, Science, 333, 719-723, https://doi.org/10.1126/science.1203752, 2011.

287 Awasthi, N., Ray, J. S., Singh, A. K., Band, S. T., and Rai, V. K.: Provenance of the Late Quaternary sediments in the
288 Andaman Sea: Implications for monsoon variability and ocean circulation, Geochem., Geophys., Geosy., 15, 3890-
289 3906, https://doi.org/10.1002/2014gc005462, 2014.

290 Ayliffe, L. K., Gagan, M. K., Zhao, J. X., Drysdale, R. N., Hellstrom, J. C., Hantoro, W. S., Griffiths, M.L., Scott-Gagan,
291 H., Pierre, E. S., Cowley, J. A., and Suwargadi, B. W.: Rapid interhemispheric climate links via the Australasian
292 monsoon during the last deglaciation, Nat. Commun., 4, 2908, https://doi.org/10.1038/ncomms3908, 2013.

293 Beck, J. W., Zhou, W., Li, C., Wu, Z., White, L., Xian, F., Kong, X. H., and An, Z.: A 550,000-year record of East Asian
294 monsoon rainfall from Be-10 in loess, Science, 360, 877-881, https://doi.org/10.1126/science.aam5825, 2018.

295 Bejugam, P., and Nayak, G. N.: Source and depositional processes of the surface sediments and their implications on
296 productivity in recent past off Mahanadi to Pennar River mouths, western Bay of Bengal, Palaeogeogr.,
297 Palaeoclimatol., Palaeoecol., 483, 58-69, https://doi.org/10.1016/j.palaeo.2016.12.006, 2017.

298 Biscaye, P. E.: Mineralogy and sedimentation of recent deep-sea clay in Atlantic Ocean and adjacent seas and oceans, Geol.
299 Soc. Amer. Bull., 76, 803-832, https://doi.org/10.1130/0016-7606(1965)76[803:masord]2.0.co;2, 1965.

300 Blaauw, M., and Christen, J. A.: Flexible Paleoclimate Age-Depth Models Using an Autoregressive Gamma Process,
301 Bayesian Analysis, 6, 457-474, https://doi.org/10.1214/11-ba618, 2011.

https://doi.org/10.5194/cp-2021-144
Preprint. Discussion started: 18 November 2021

302 Broccoli, A. J., Dahl, K. A., and Stouffer, R. J.: Response of the ITCZ to Northern Hemisphere cooling, Geophys. Res.
303 Lett., 33, L01702, https://doi.org/10.1029/2005GL024546, 2006.
304 Chamley, H.: Clay Sedimentology, Springer, Berlin, 623 pp., 1989.
305 Chatterjee, A., Shankar, D., McCreary, J. P., Vinayachandran, P. N., and Mukherjee, A.: Dynamics of Andaman Sea
306 circulation and its role in connecting the equatorial Indian Ocean to the Bay of Bengal, J. Geophys. Res. Oceans, 122,
307 3200-3218, https://doi.org/10.1002/2016JC012300, 2017.
308 Colin, C., Turpin, L., Bertaux, J., Desprairies, A., and Kissel, C.: Erosional history of the Himalayan and Burman Ranges
309 during the last two glacial-interglacial cycles, Earth Planet. Sci. Lett., 171, 647–660, https://doi.org/10.1016/s0012-
310 821x(99)00184-3, 1999.
311 Colin, C., Turpin, L., Blamart, D., Frank, N., Kissel, C., and Duchamp, S.: Evolution of weathering patterns in the Indo-
312 Burman Ranges over the last 280 kyr: Effects of sediment provenance on $^{87}Sr/^{86}Sr$ ratios tracer, Geochem., Geophys.,
313 Geosy., 7, Q03007, https://doi.org/10.1029/2005gc000962, 2006.
314 Curray, J. R., Emmel, F. J., and Moore, D. G.: The Bengal Fan: morphology, geometry, stratigraphy, history and processes,
315 Mar. Petrol. Geol., 19, 1191-1223, https://doi.org/10.1016/S0264-8172(03)00035-7, 2002.
316 Deplazes, G., Lückge, A., Peterson, L. C., Timmermann, A., Hamann, Y., Hughen, K. A., Röhl, U., Laj, C., Cane, M. A.,
317 Sigman, D. M., and Haug, G. H.: Links between tropical rainfall and North Atlantic climate during the last glacial
318 period, Nat. Geosci., 6, 213-217, https://doi.org/10.1038/ngeo1712, 2013.
319 DiNezio, P. N., and Tierney, J. E.: The effect of sea level on glacial Indo-Pacific climate, Nat. Geosci., 6, 485-491,
320 https://doi.org/10.1038/ngeo1823, 2013.
321 Dutt, S., Gupta, A. K., Clemens, S. C., Cheng, H., Singh, R. K., Kathayat, G., and Edwards, R. L.: Abrupt changes in Indian
322 summer monsoon strength during 33,800 to 5500 years B.P., Geophys. Res. Lett., 42, 5526-5532,
323 https://doi.org/10.1002/2015gl064015, 2015.

https://doi.org/10.5194/cp-2021-144
Preprint. Discussion started: 18 November 2021

Erosion, H. S.: Sedimentation and sedimentary origin of clays, in: Velde, B. (Ed.), Origin and Mineralogy of Clays. Clays Environment., Springer, Berlin, pp. 162–219, 1995.

Fournier, L., Fauquembergue, K., Zaragosi, S., Zorzi, C., Malaize, B., Bassinot, F., Joussain, R., Colin, C., Moreno, E., and Leparmentier, F.: The Bengal fan: external controls on the Holocene Active Channel turbidite activity, Holocene, 27 (6), 900-913, https://doi.org/10.1177/0959683616675938, 2017.

Gautam, P. K., Narayana, A. C., Kumar, P. K., Bhavani, P. G., Yadava, M. G., and Jull, A. J. T.: Indian monsoon variability during the last 46 kyr: isotopic records of planktic foraminifera from southwestern Bay of Bengal, J. Quat. Sci., 36, 138-151, https://doi.org/10.1002/jqs.3263, 2020.

Gebregiorgis, D., Hathorne, E. C., Sijinkumar, A. V., Nath, B. N., Nürnberg, D., and Frank, M.: South Asian summer monsoon variability during the last ~54 kyrs inferred from surface water salinity and river runoff proxies, Quat. Sci. Rev., 138, 6-15, https://doi.org/10.1016/j.quascirev.2016.02.012, 2016.

Gibbs, R. J.: Clay mineral segregation in the marine environment, J. Sediment. Res., 47, 237-243, 1977.

Goodbred, S. L., and Kuehl, S. A.: Enormous Ganges-Brahmaputra sediment discharge during strengthened early Holocene monsoon, Geology, 28, 1083-1086, https://doi.org/10.1130/0091-7613(2000)028<1083:Egbsdd>2.3.Co;2, 2000.

Grant, K. M., Rohling, E. J., Ramsey, C. B., Cheng, H., Edwards, R. L., Florindo, F., Heslop, D., Marra, F., Roberts, A. P., Tamisiea, M. E., and Williams, F.: Sea-level variability over five glacial cycles, Nat. Commun., 5, 5076, https://doi.org/10.1038/ncomms6076, 2014.

Hanebuth, T., Stattegger, K., and Grootes, P. M.: Rapid Flooding of the Sunda Shelf: A Late-Glacial Sea-Level Record, Science, 288, 1033-1035, https://doi.org/10.1126/science.288.5468.1033, 2000.

Huang, J., Wan, S., Li, A., and Li, T.: Two-phase structure of tropical hydroclimate during Heinrich Stadial 1 and its global implications, Quat. Sci. Rev., 222, 105900, https://doi.org/10.1016/j.quascirev.2019.105900, 2019.

Jacobsen, S. B. and Wasserburg, G. J.: Sm-Nd isotopic evolution of chondrites, Earth Planet. Sci. Lett., 50, 139-155,

https://doi.org/10.5194/cp-2021-144
Preprint. Discussion started: 18 November 2021

https://doi.org/10.1016/0012-821x(80)90125-9, 1980.

Joussain, R., Colin, C., Liu, Z., Meynadier, L., Fournier, L., Fauquembergue, K., Zaragosi, S., Schmidt, F., Rojas, V., and Bassinot, F.: Climatic control of sediment transport from the Himalayas to the proximal NE Bengal Fan during the last glacial-interglacial cycle, Quat. Sci. Rev., 148, 1-16, https://doi.org/10.1016/j.quascirev.2016.06.016, 2016.

Joussain, R., Liu, Z., Colin, C., Duchamp-Alphonse, S., Yu, Z., Moréno, E., Fournier, L., Zaragosi, S., Dapoigny, A., Meynadier, L., and Bassinot, F.: Link between Indian monsoon rainfall and physical erosion in the Himalayan system during the Holocene, Geochem., Geophys., Geosy., 18, 3452-3469, https://doi.org/10.1002/2016gc006762, 2017.

Kessarkar, P. M., Rao, V. P., Ahmad, S. M., Patil, S. K., Kumar, A. A., Babu, G. A., Chakraborty, S., and Rajan, R. S.: Changing sedimentary environment during the Late Quaternary: Sedimentological and isotopic evidence from the distal Bengal Fan, Deep Sea Res. Pt I: Oceanogr. Res. Papers, 52, 1591-1615, https://doi.org/10.1016/j.dsr.2005.01.009, 2005.

Khan, M. H. R., Liu, J., Liu, S., Seddique, A. A., Cao, L., and Rahman, A.: Clay mineral compositions in surface sediments of the Ganges-Brahmaputra-Meghna river system of Bengal Basin, Bangladesh, Mar. Geol., 412, 27-36, https://doi.org/10.1016/j.margeo.2019.03.007, 2019.

Li, J., Liu, S., Shi, X., Feng, X., Fang, X., Cao, P., Sun, X. Q., Ye, W. X., Khokiattiwong, S., and Kornkanitnan, N.: Distributions of clay minerals in surface sediments of the middle Bay of Bengal: Source and transport pattern, Continent. Shelf Res., 145, 59-67, https://doi.org/10.1016/j.csr.2017.06.017, 2017.

Li, J., Liu, S., Shi, X., Zhang, H., Fang, X., Chen, M.-T., Cao, P., Sun, X. Q., Ye, W. X., Wu, K. K., Khokiattiwong, S., and Kornkanitnan, N.: Clay minerals and Sr-Nd isotopic composition of the Bay of Bengal sediments: Implications for sediment provenance and climate control since 40 ka, Quat. Internat., 493, 50-58, https://doi.org/10.1016/j.quaint.2018.06.044, 2018.

Licht, A. France-Lanord, C., Reisberg, L., Fontaine, C., Soe, A. N., and Jaeger, J. J.: A palaeo Tibet-Myanmar connection?

https://doi.org/10.5194/cp-2021-144
Preprint. Discussion started: 18 November 2021

368 Reconstructing the Late Eocene drainage system of central Myanmar using a multi-proxy approach, J. Geol. Soc.,
369 170, 929-939, https://doi.org/10.1144/jgs2012-126, 2013.
370 Liu, J., He, W., Cao, L., Zhu, Z., Xiang, R., Li, T., Shi, X., and Liu, S.: Staged fine-grained sediment supply from the
371 Himalayas to the Bengal Fan in response to climate change over the past 50,000 years, Quat. Sci. Rev., 212, 164-177,
372 https://doi.org/10.1016/j.quascirev.2019.04.008, 2019a.
373 Liu, J., Zhu, Z., Xiang, R., Cao, L., He, W., Liu, S., and Shi, X.: Geochemistry of core sediments along the Active Channel,
374 northeastern Indian Ocean over the past 50,000 years: Sources and climatic implications, Palaeogeogr.,
375 Palaeoclimatol., Palaeoecol., 521, 151-160, https://doi.org/10.1016/j.palaeo.2019.02.021, 2019b.
376 Liu, J. P., Kuehl, S. A., Pierce, A. C., Williams, J., Blair, N. E., Harris, C., Aung, D. W., and Aye, Y. Y.: Fate of Ayeyarwady
377 and Thanlwin Rivers Sediments in the Andaman Sea and Bay of Bengal, Mar. Geol., 423, 106137,
378 https://doi.org/10.1016/j.margeo.2020.106137, 2020a.
379 Liu, S., Li, J., Zhang, H., Cao, P., Mi, B., Khokiattiwong, S., Kornkanitnan, N., and Shi, X.: Complex response of
380 weathering intensity registered in the Andaman Sea sediments to the Indian Summer Monsoon over the last 40 kyr,
381 Mar. Geol., 426, 106206, https://doi.org/10.1016/j.margeo.2020.106206, 2020b.
382 Liu, S., Ye, W., Cao, P., Zhang, H., Chen, M. -T., Li, X., Li, J., Pan, H.-J., Khokiattiwong, S., Kornkanitnan, N., and Shi,
383 X.: Paleoclimatic responses in the tropical Indian Ocean to regional monsoon and global climate change over the last
384 42 kyr, Mar. Geol., 438, 106542, https://doi.org/10.1016/j.margeo.2021.106542, 2021.
385 Liu, Z., Wang, H., Hantoro, W. S., Sathiamurthy, E., Colin, C., Zhao, Y., Li, J.: Climatic and tectonic controls on chemical
386 weathering in tropical Southeast Asia (Malay Peninsula, Borneo, and Sumatra), Chem. Geol., 291, 1-12,
387 https://doi.org/10.1016/j.chemgeo.2011.11.015, 2012.
388 Lupker, M., France-Lanord, C., Galy, V., Lavé, J., and Kudrass, H.: Increasing chemical weathering in the Himalayan
389 system since the Last Glacial Maximum, Earth Planet. Sci. Lett., 365, 243-252,

https://doi.org/10.5194/cp-2021-144
Preprint. Discussion started: 18 November 2021

https://doi.org/10.1016/j.epsl.2013.01.038, 2013.

McGee, D., Moreno-Chamarro, E., Green, B., Marshall, J., Galbraith, E., and Bradtmiller, L.: Hemispherically asymmetric trade wind changes as signatures of past ITCZ shifts, Quat. Sci. Rev., 180, 214-228, https://doi.org/10.1016/j.quascirev.2017.11.020, 2018.

Mohtadi, M., Prange, M., Oppo, D. W., De Pol-Holz, R., Merkel, U., Zhang, X., Steinke, S., and Luckge, A.: North Atlantic forcing of tropical Indian Ocean climate, Nature, 509, 76-80, https://doi.org/10.1038/nature13196, 2014.

Mohtadi, M., Prange, M., Schefuss, E., and Jennerjahn, T. C.: Late Holocene slowdown of the Indian Ocean Walker circulation, Nat. Commun., 8, 1015, https://doi.org/10.1038/s41467-017-00855-3, 2017.

Niedermeyer, E. M., Sessions, A. L., Feakins, S. J., and Mohtadi, M.: Hydroclimate of the western Indo-Pacific Warm Pool during the past 24,000 years, Proc. Nation. Acad. Sci., 111, 9402-9406, https://doi.org/10.1073/pnas.1323585111, 2014.

Peng, J., Yang, X., Toney, J. L., Ruan, J., Li, G., Zhou, Q., Gao, H., Xie, Y., Chen, Q., and Zhang, T.: Indian Summer Monsoon variations and competing influences between hemispheres since ~35 ka recorded in Tengchongqinghai Lake, southwestern China, Palaeogeogr., Palaeoclimatol., Palaeoecol., 516, 113-125, https://doi.org/10.1016/j.palaeo.2018.11.040, 2019.

Prajith, A., Tyagi, A., and John Kurian, P.: Changing sediment sources in the Bay of Bengal: Evidence of summer monsoon intensification and ice-melt over Himalaya during the Late Quaternary, Palaeogeogr., Palaeoclimatol., Palaeoecol., 511, 309-318, https://doi.org/10.1016/j.palaeo.2018.08.016, 2018.

Rashid, H., England, E., Thompson, L., and Polyak, L.: Late Glacial to Holocene Indian Summer Monsoon Variability Based upon Sediment Records Taken from the Bay of Bengal, Terr., Atmosp. Ocean. Sci., 22, 215-228, https://doi.org/10.3319/TAO.2010.09.17.02(TibXS), 2011.

Rayaroth, M. K., Peter, B. N., and Mahmud, M. R.: High-resolution surface circulation of the Bay of Bengal derived from

https://doi.org/10.5194/cp-2021-144
Preprint. Discussion started: 18 November 2021

412 satellite observation data, J. Mar. Sci. Technol., 24, 656-668, https://doi.org/10.6119/JMST-015-1215-2, 2016.

413 Raza, T., and Ahmad, S. M.: Surface and deep water variations in the northeast Indian Ocean during 34-6 ka BP: evidence
414 from carbon and oxygen isotopes of fossil foraminifera, Quat. Internat., 298, 37-44,
415 https://doi.org/10.1016/j.quaint.2012.05.005, 2013.

416 Reimer, P. J., Austin, W. E. N., Bard, E., Bayliss, A., Blackwell, P. G., Bronk Ramsey, C., Butzin, M., Cheng, H., Edwards,
417 R.L., Friedrich, M., Grootes, P. M., Guilderson, T. P., Hajdas, I., Heaton, T. J., Hogg, A. G., Hughen, K. A., Kromer,
418 B., Manning, S. W., Muscheler, R., Palmer, J. G., Pearson, C., van der Plicht, J., Reimer, R. W., Richards, D. A., Scott,
419 E. M., Southon, J. R., Turney, C. S. M., Wacker, L., Adolphi, F., Büntgen, U., Capano, M., Fahrni, S. M., Fogtmann-
420 Schulz, A., Friedrich, R., Köhler, P., Kudsk, S., Miyake, F., Olsen, J., Reinig, F., Sakamoto, M., Sookdeo, A., and
421 Talamo, S.: The intcal20 northern hemisphere radiocarbon age calibration curve (0-55 cal kBP), Radiocarbon, 62,
422 725-757, https://doi.org/10.1017/RDC.2020.41, 2020.

423 Rodolfo, K. S.: Sediments of Andaman Basin, northeastern Indian Ocean, Mar. Geol., 7, 371-380,
424 https://doi.org/10.1016/0025-3227(69)90014-0, 1969.

425 Schneider, T., Bischoff, T., and Haug, G. H.: Migrations and dynamics of the intertropical convergence zone, Nature, 513,
426 45-53, https://doi.org/10.1038/nature13636, 2014.

427 Schott, F. A., and McCreary, J. P.: The monsoon circulation of the Indian Ocean, Progr. Oceanogr., 51, 1-123,
428 https://doi.org/10.1016/s0079-6611(01)00083-0, 2001.

429 Shankar, D., Vinayachandran, P. N., and Unnikrishnan, A. S.: The monsoon currents in the north Indian Ocean,Progr.
430 Oceanogr., 52, 63-120, https://doi.org/10.1016/s0079-6611(02)00024-1, 2002.

431 Stoll, H. M., Vance, D., and Arevalos, A.: Records of the Nd isotope composition of seawater from the Bay of Bengal:
432 Implications for the impact of Northern Hemisphere cooling on ITCZ movement, Earth Planet. Sci. Lett., 255, 213-
433 228, https://doi.org/10.1016/j.epsl.2006.12.016, 2007

https://doi.org/10.5194/cp-2021-144
Preprint. Discussion started: 18 November 2021

434 Svensson, A., Andersen, K. K., Bigler, M., Clausen, H. B., Dahl-Jensen, D., Davies, S. M., Johnsen, S. J., Muscheler, R.,
435 Parrenin, F., Rasmussen, S. O., Röthlisberger, R., Seierstad, I., Steffensen, J. P., and Vinther, B. M.: A 60 000 year
436 Greenland stratigraphic ice core chronology, Clim. Past, 4, 47-57, https://doi.org/10.5194/cp-4-47-2008, 2008
437 Tan, L., Shen, C. C., Lowemark, L., Chawchai, S., Edwards, R. L., Cai, Y., Breitenbach, S. F. M., Cheng, H., Chou, Y. C.,
438 Duerrast, H., Partin, J. W., Cai, W., Chabangborn, A., Gao, Y., Kwiecien, O., Wu, C. C., Shi, Z., Hsu, H. H., and
439 Wohlfarth, B.: Rainfall variations in central Indo-Pacific over the past 2,700 y, Proc. Nation. Acad. Sci., 116, 17201-
440 17206, https://doi.org/10.1073/pnas.1903167116, 2019.
441 Thompson, W. G., and Goldstein, S. L.: A radiometric calibration of the SPECMAP timescale, Quat. Sci. Rev., 25, 3207-
442 3215, https://doi.org/10.1016/j.quascirev.2006.02.007, 2006.
443 Tripathy, G. R., Singh, S. K., and Bhushan, R.: Sr-Nd isotope composition of the Bay of Bengal sediment impact of climate
444 on erosion in the Himalaya, Geochem. J., 45, 175-186, 2011.
445 Tripathy, G. R., Singh, S. K., and Ramaswamy, V.: Major and trace element geochemistry of Bay of Bengal sediments:
446 Implications to provenances and their controlling factors, Palaeogeogr., Palaeoclimatol., Palaeoecol., 397, 20-30,
447 https://doi.org/10.1016/j.palaeo.2013.04.012, 2014.
448 Turner, S., and Foden, J.: U, Th and Ra disequilibria, Sr, Nd and Pb isotope and trace element variations in Sunda arc lavas:
449 predominance of a subducted sediment component, Contr. Mineral. Petrol., 142, 43-57,
450 https://doi.org/10.1007/s004100100271, 2001.
451 Waelbroecka, C., Labeyrieab, L., Michela, E., Duplessya, J. C., McManusc, J. F., Lambeckd, K., Balbona, E., and
452 Labracherie, M.: Sea-level and deep water temperature changes derived from benthic foraminifera isotopic records,
453 Quat. Sci. Rev., 21, 295-305, https://doi.org/10.1016/s0277-3791(01)00101-9, 2002.
454 Weldeab, S., Rühlemann, C., Bookhagen, B., Pausata, F. S. R., and Perez‐Lua, F. M.: Enhanced Himalayan Glacial
455 Melting During YD and H1 Recorded in the Northern Bay of Bengal, Geochem., Geophys., Geosy., 20, 2449-2461,

https://doi.org/10.5194/cp-2021-144
Preprint. Discussion started: 18 November 2021

https://doi.org/10.1029/2018GC008065, 2019.

Winkler, A., Wolf-Welling, T., Stattegger, K., and Thiede, J.: Clay mineral sedimentation in high northern latitude deep-sea basins since the Middle Miocene (ODP Leg 151, NAAG), Interna. J. Earth Sci., 91 (1), 133–148, https://doi.org/10.1007/s005310100199, 2002.

Yan, Q., Owen, L. A., Zhang, Z., Jiang, N., and Zhang, R.: Deciphering the evolution and forcing mechanisms of glaciation over the Himalayan-Tibetan orogen during the past 20,000 years, Earth Planet. Sci. Lett., 541, 116295, https://doi.org/10.1016/j.epsl.2020.116295, 2020.

Ye, W., Liu, S., Fan, D., Zhang, H., Cao, P., Pan, H. -J., Li, J., Li, X., Fang, X., Khokiattiwong, S., Kornkanitnan, N., and Shi, X.: Evolution of sediment provenances and transport processes in the central Bay of Bengal since the Last Glacial Maximum, Quat. Internat., (in press). https://doi.org/10.1016/j.quaint.2020.12.007, 2020.

Yu, Z., Colin, C., Wan, S., Saraswat, R., Song, L., Xu, Z., Clift, P., Lu, H., Lyle, M., Kulhanek, D., Hahn, A., Tiwari, M., Mishra, R., Miska, S., and Kumar, A.: Sea level-controlled sediment transport to the eastern Arabian Sea over the past 600 kyr: clay minerals and Sr-Nd isotopic evidence from IOD site U1457, Quat. Sci. Rev., 205, 22-34, https://doi.org/10.1016/j.quascirev.2018.12.006, 2019.

Zhang, X., Zheng, Z., Huang, K., Yang, X., and Tian, L.: Sensitivity of altitudinal vegetation in southwest China to changes in the Indian summer monsoon during the past 68000 years, Quat. Sci. Rev., 239, 106359, https://doi.org/10.1016/j.quascirev.2020.106359, 2020.

Zhuravleva, A., Hüls, M., Tiedemann, R., and Bauch, H. A.: A 125-ka record of northern South American precipitation and the role of high-to-low latitude teleconnections, Quat. Sci. Rev., 270, 107159, https://doi.org/10.1016/j.quascirev.2021.107159, 2021.

Zorzi, C., Sanchez Goñi, M. F., Anupama, K., Prasad, S., Hanquiez, V., Johnson, J., and Giosan, L.: Indian monsoon variations during three contrasting climatic periods: The Holocene, Heinrich Stadial 2 and the last interglacial–glacial

https://doi.org/10.5194/cp-2021-144
Preprint. Discussion started: 18 November 2021

478 transition, Quat. Sci. Rev., 125, 50-60, https://doi.org/10.1016/j.quascirev.2015.06.009, 2015.

479 **Figure Captions**

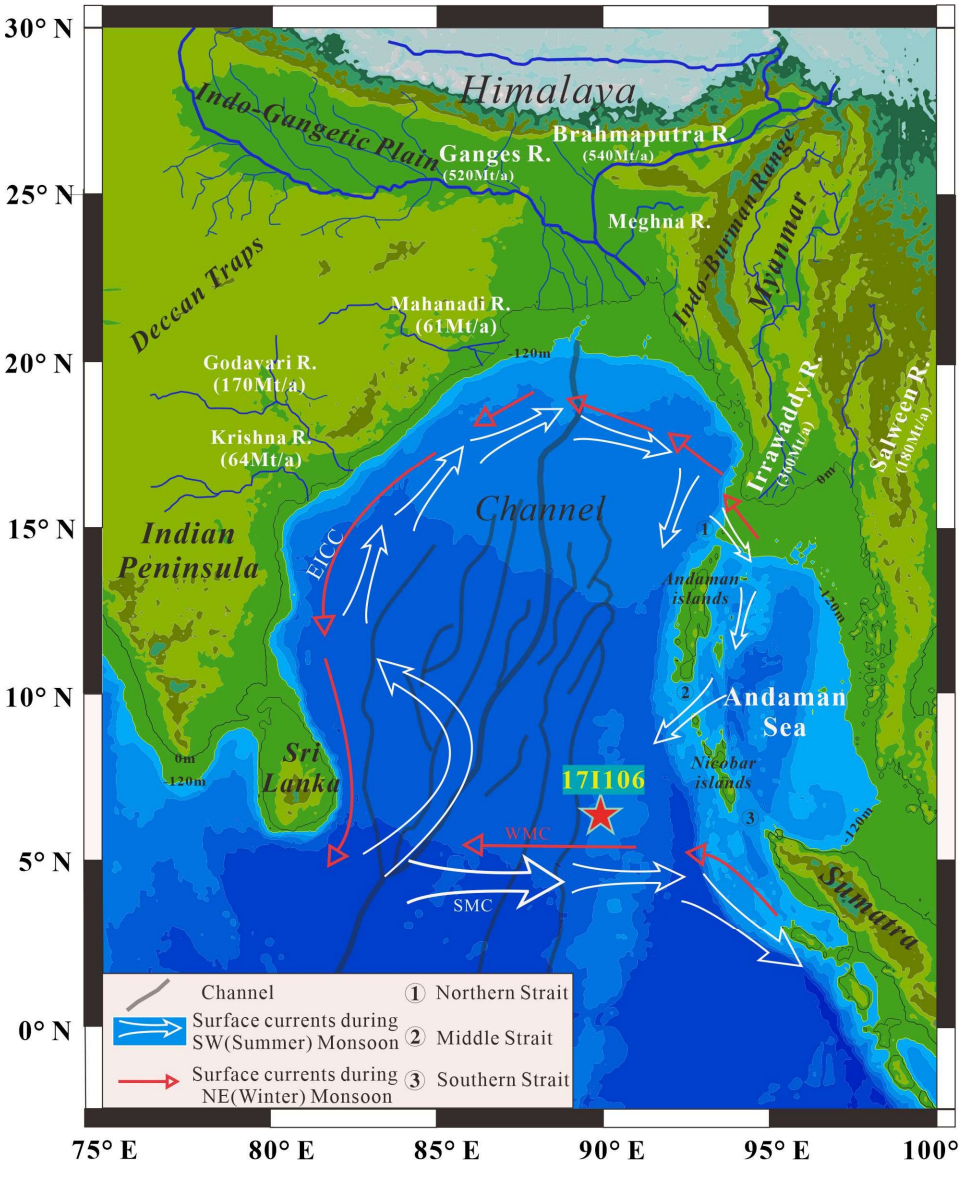

480

481 **Figure 1.** Geographical setting and hydrography in the BoB. The locations of core 17I106 (red asterisks) are shown. The

482 white and red arrows denote the SW and NE monsoon currents, respectively. In the western BoB, the East Indian Coastal

https://doi.org/10.5194/cp-2021-144
Preprint. Discussion started: 18 November 2021

Climate of the Past Discussions
Open Access
EGU

Current (EICC) reverses annually with the monsoon wind (Schott and McCreary, 2001). In the lower-latitude regions of the BoB, monsoon-driven currents flow eastward in summer to form the summer monsoon current (SMC) and westward in winter to form the winter monsoon current (WMC) (Shankar et al., 2002).

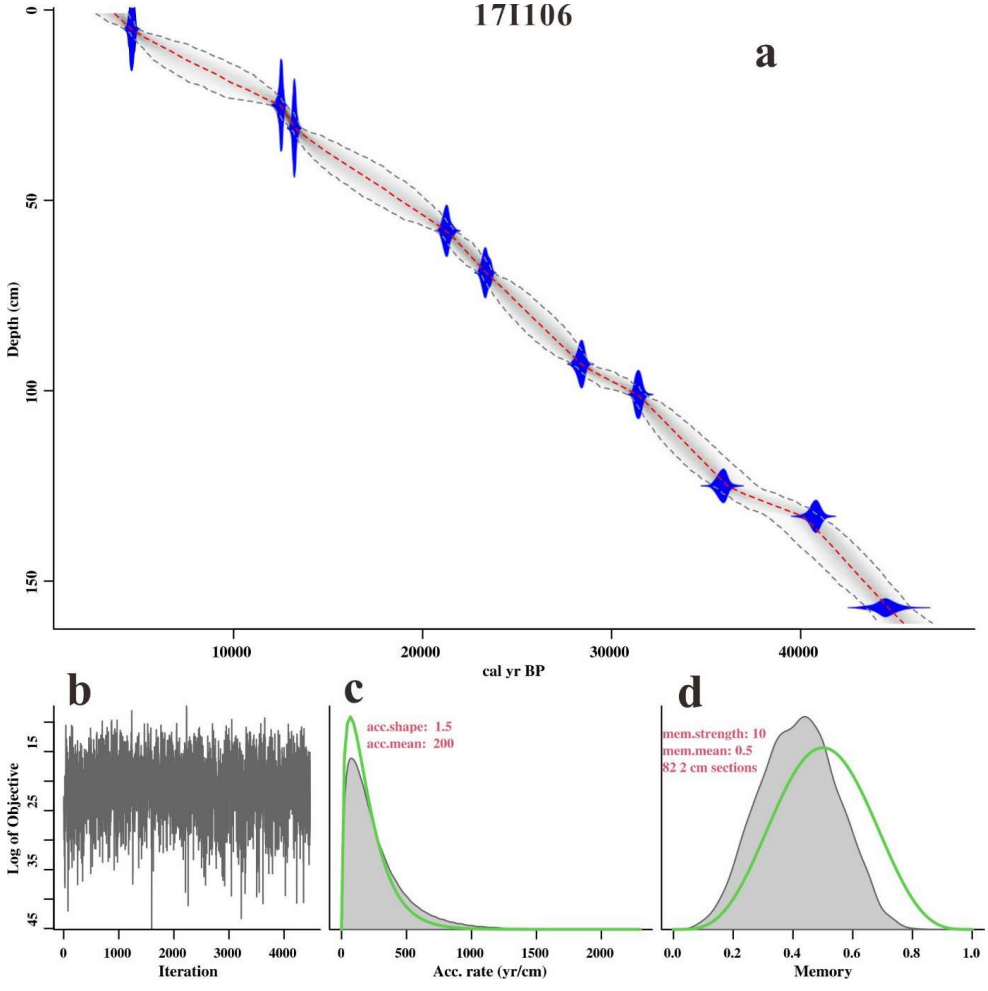

Figure 2. Age-depth model of core 17I106 in the northeastern Indian Ocean. **a,** Calibrated ^{14}C dates (blue, with 2σ errors) and the resulting age-depth model (the darker gray shading indicates more likely calendar ages; the gray stippled lines show 95% confidence intervals; and the red curve shows the single 'best' model based on the weighted mean age for each depth). **b,** Number of Markov chain Monte Carlo (MCMC) iterations used to generate the grayscale graphs. **c,** Prior (green) and posterior (gray) distributions of the sediment accumulation rates (the mean sediment accumulation rate was ~2

https://doi.org/10.5194/cp-2021-144
Preprint. Discussion started: 18 November 2021

Climate of the Past Discussions
Open Access
EGU

492 years/cm). **d,** Prior (green) and posterior (gray) memory distributions (dependence of the sediment accumulation rate

493 between neighboring depths).

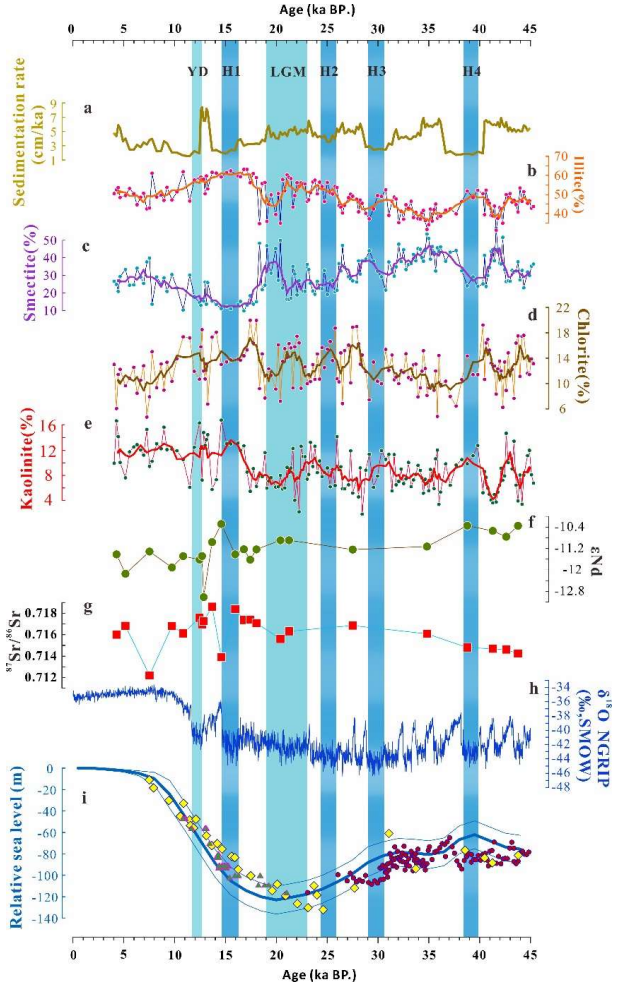

494

495 **Figure 3.** Comparison of clay mineral and Sr-Nd isotopes data in the northeastern Indian Ocean with paleoclimate records.

496 **a**, Sedimentation rate in core 17I106; **b, c, d, e**, illite, smectite, chlorite and kaolinite percentages in core 17I106 (thick line

497 represents a 3-point running average); **f, g** $^{87}Sr/^{86}Sr$ and εNd values of core 17I106 in the northeastern Indian Ocean; **h**,

498 $\delta^{18}O$ data of Greenland ice core NGRIP; **i**, Global sea level as proxy for ice volume, reconstructed from benthic $\delta^{18}O$ (thick

499 cyan line, thin cyan line represents the 95% confidence interval, Thompson and Goldstein, 2006), globally distributed

https://doi.org/10.5194/cp-2021-144
Preprint. Discussion started: 18 November 2021

Climate of the Past Discussions
Open Access
EGU

500 corals (yellow dots, Waelbroecka et al., 2002) and sea level data (Triangles and red dots) collect by Grant et al.(2014) and
501 Hanebuth et al. (2000). Blue and cyan bars represent cold climate periods of Heinrich events (H1-H4) together with
502 Younger Dryas (YD) and last glacial maximum (LGM), respectively.

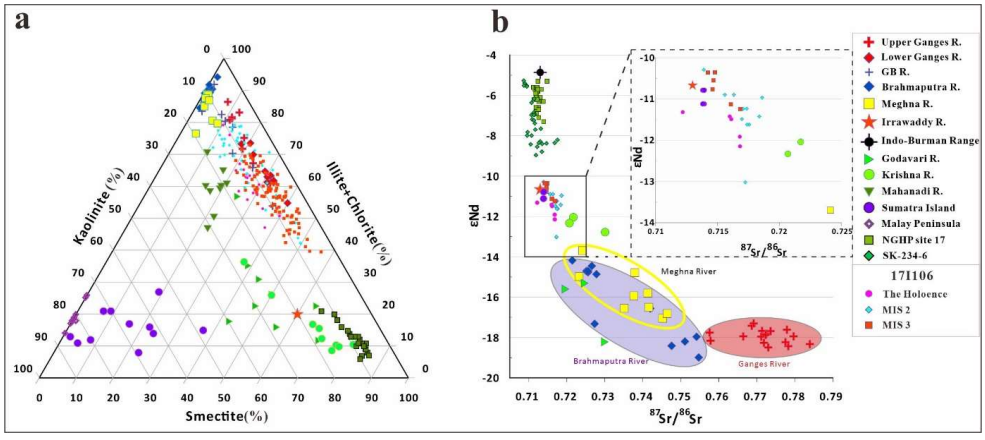

503

504 **Figure 4.** Sediment provenance of core 17I106 in the northeastern Indian Ocean. **a**, Sediment provenance discrimination
505 diagram in the northeastern Indian Ocean. For comparison, clay mineral data obtained from sediments collected in the
506 modern Ganges River, Brahmaputra River Lower, Ganges-Brahmaputra River Lower and Meghna River (Khan et al., 2019),
507 Mahanadi and Krishna Rivers of Indian Peninsula (Bejugam and Nayak, 2017), Irrawaddy River (Rodolfo, 1969), and
508 Sumatra and Malay Peninsula rivers (Liu et al., 2012) are also plotted. The referenced cores comprise NGHP Site 17 (Ali
509 et al., 2015), representing the Irrawaddy River as main clay mineral source in the Andaman Sea. **b**, Variations in εNd (0)
510 vs. $^{87}Sr/^{86}Sr$ measured in core 17I106 compared with those measured in river sediments and bulk rock samples collected
511 around the BoB. In this diagram, we display data collected from Indian river samples (from the Godavari and Krishna
512 Rivers) (Ahmad et al., 2009), from different parts of the modern G-B River system (Lupker et al., 2013). Measurements
513 taken from sediments obtained from the Irrawaddy River (Colin et al., 1999), formations from the Indo-Burman ranges
514 (Licht et al., 2013) and volcanic products of Sumatra Island (Turner et al., 2001) are also plotted. The referenced cores
515 include NGHP Sites 17 and SK-234-60, both of which indicate that the Irrawaddy River is the main Sr-Nd isotope source
516 for the Andaman Sea.

https://doi.org/10.5194/cp-2021-144
Preprint. Discussion started: 18 November 2021

Climate of the Past Discussions
Open Access
EGU

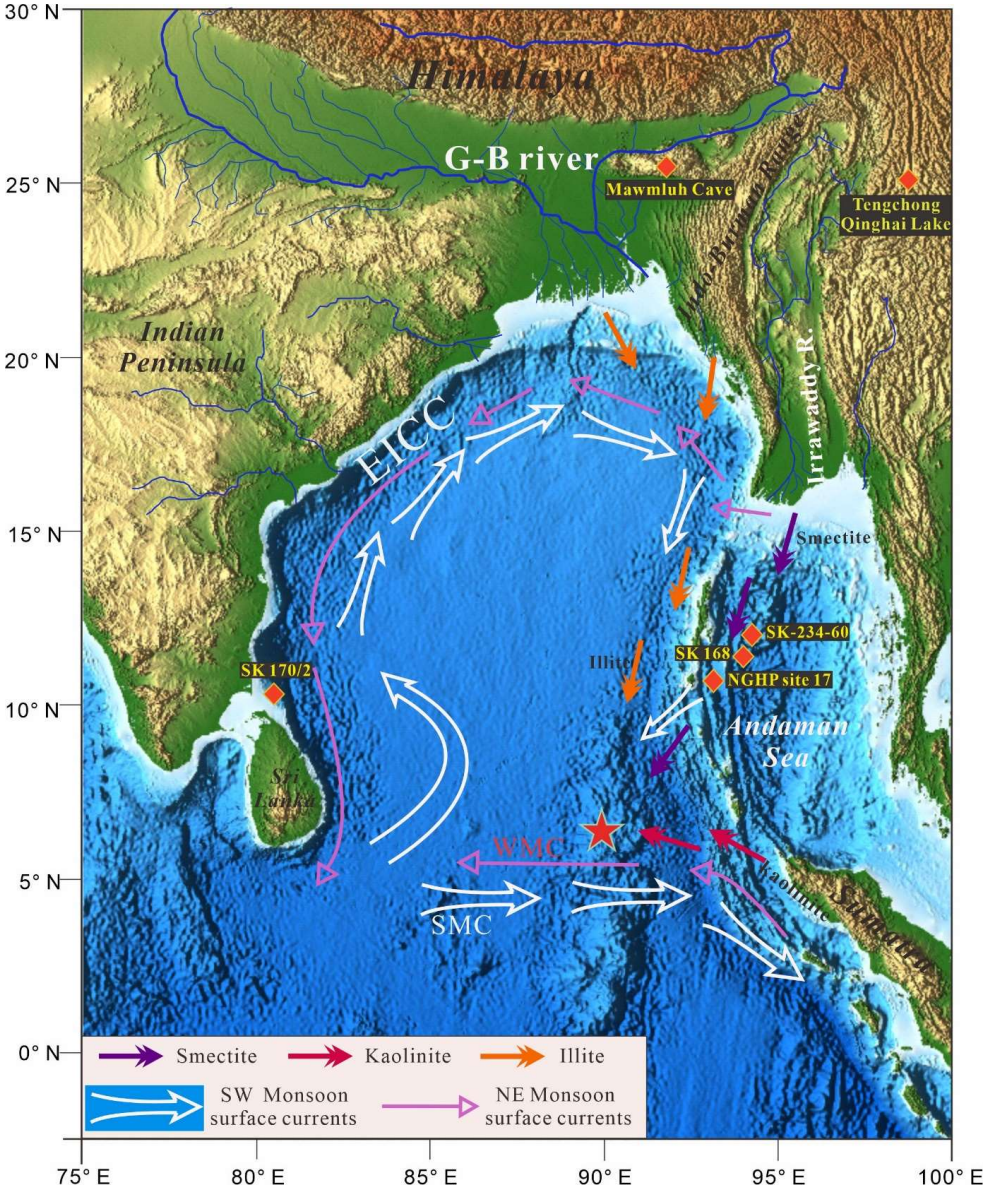

Figure 5. Map showing dispersal patterns of the BoB clay minerals for core 17I106. The locations of core 17I106 (red asterisks), and of the referenced core and sites are shown: SK 170/2 in the northern BoB, SK-168, SK-234-60, NGHP site 17 in the western Andaman Sea, and Mawmluh Cave in northeastern India and Tengchong Qinghai Lake in China are represented by Orange diamond. The orange, purple and red arrows represent the main dispersal directions of illite, smectite

https://doi.org/10.5194/cp-2021-144
Preprint. Discussion started: 18 November 2021

Climate of the Past Discussions
Open Access
EGU

522 and kaolinite when the fluvial sediments were discharged into the core 17I106.

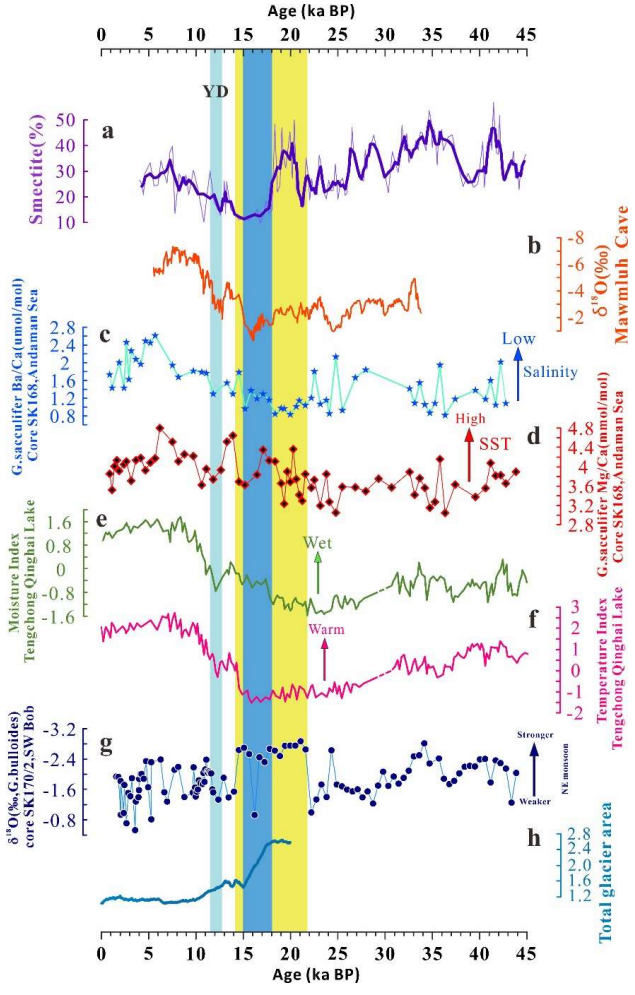

523

524 **Figure 6.** Comparison of smectite percentage in core 17I106 with paleoclimate records. **a**, smectite percentages in core

525 17I106 (thick line represents a 3-point running average); **b,** Mawmluh Cave $\delta^{18}O$ record for the interval 33,800 to 5500

526 years BP (Dutt et al., 2015).**c, d,** Ba/Ca and Mg/Ca of the mixed layer species *G. sacculifer* in core SK 168 from Andaman

527 sea, which represent the surface sea salinity and temperature, and the lower salinity and higher temperature showed strong

528 SW monsoon (Gebregiorgis et al., 2016).**e, f,** Moisture index and temperature index form pollen records from Tengchong

529 Qinghai Lake, respectively (Zhang et al., 2020).**g,** $\delta^{18}O$ variability record of planktic foraminifera *Orbulina universa*

https://doi.org/10.5194/cp-2021-144
Preprint. Discussion started: 18 November 2021

Climate of the Past Discussions
Open Access
EGU

530 obtained from core SK-170/2 recovered from the southwestern Bay of Bengal, which represent the strength of NE
531 monsoon(Gautam et al., 2020).**h,** Ratio of the modeled total glacier area over the southern parts of the Himalayan-Tibetan
532 orogen to present level (Yan et al., 2020).Yellow, blue and cyan bars represent strong NE monsoon period showed by line
533 **g**, main periods of glacier melting in the southern Himalayas showed by line **h** and cold climate periods of Younger Dryas
534 (YD).

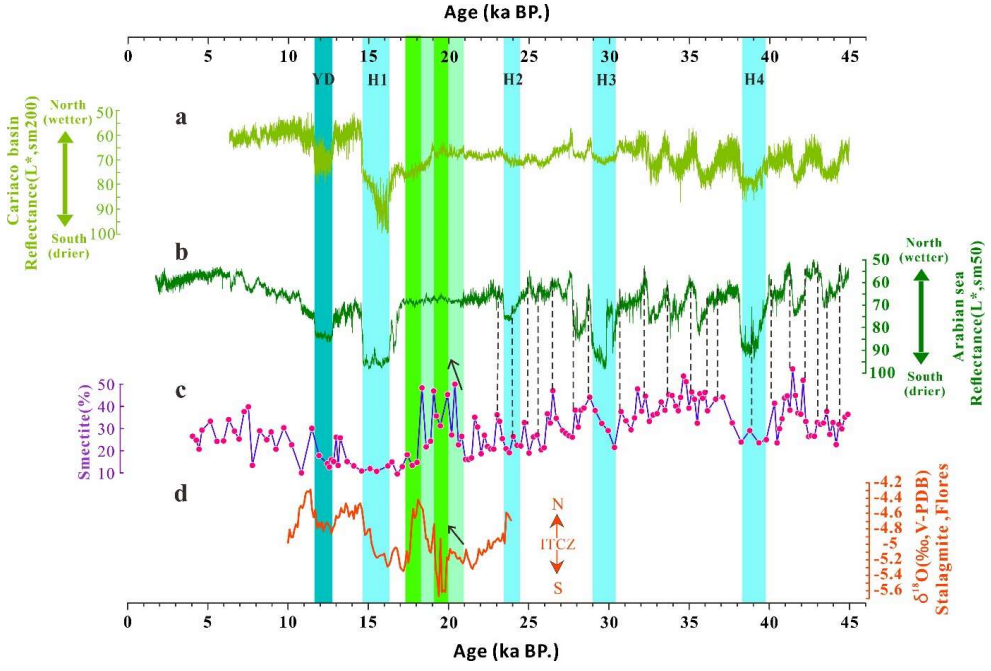

535

536 **Figure 7.** Comparison of smectite percentages with ITCZ north-south shift records. **a,** L* represents the ITCZ shift from
537 the Cariaco Basin (Deplazes et al., 2013); **b**, L* represents the ITCZ shift from the Arabian Sea (Deplazes et al., 2013); **c**,
538 Smectite percentages in core 17I106; **d**, Stalagmite $\delta^{18}O$ record from Flores (Ayliffe et al., 2013). The gold dotted line
539 denotes the connection between the northward movement of the ITCZ and the peak smectite percentage, and the series of
540 color bars from 21-18 ka represent the ITCZ-shift periods recorded in **d.** The green bars represent the consistent periods
541 shown in **c** and **d** in the late LGM, and the black arrows in **c** and **d** indicate great differences between the smectite
542 percentages and ITCZ record in the EIO.

https://doi.org/10.5194/cp-2021-144
Preprint. Discussion started: 18 November 2021

Climate of the Past Discussions
Open Access
EGU

543 **Table 1.** Carbon-14 and calibrated calendar ages of mixed planktonic foraminifera measured in core 17I106 in the

544 northeastern Indian Ocean.

Number	Depth (cm)	Materials	Measured ^{14}C age (yr BP, ±1σ)	Calendar median age (yr BP)
1	5	mixed planktonic foraminifera	4160±30	4053
2	25	mixed planktonic foraminifera	10690±40	11880
34	31	mixed planktonic foraminifera	11460±40	12801
4	58	mixed planktonic foraminifera	17910±50	20710
5	69	mixed planktonic foraminifera	20050±60	23183
6	93	mixed planktonic foraminifera	24590±90	27883
7	101	mixed planktonic foraminifera	27820±120	31074
8	125	mixed planktonic foraminifera	31820±200	35455
9	133	mixed planktonic foraminifera	36370±280	40434
10	157	mixed planktonic foraminifera	42190±560	44167

545